

## Targeted recovery of metals from Thermoelectric Generators (TEGs) using chloride brines and ultrasound

Guillaume Zante<sup>\*,a</sup>, Evangelia Daskalopoulou<sup>a</sup>, Christopher E. Elgar<sup>a</sup>, Rodolfo Marin Rivera<sup>a</sup>, Jennifer M. Hartley<sup>a</sup>, Kevin Simpson<sup>b</sup>, Richard Tuley<sup>b</sup>, Jeff Kettle<sup>c</sup>, Andrew P. Abbott<sup>a</sup>

<sup>a</sup> School of Chemistry, University of Leicester, Leicester, LE1 7RH, UK

<sup>b</sup> European Thermodynamics Ltd., Kibworth, LE8 0RX, UK

<sup>c</sup> James Watt School of Engineering, University of Glasgow, Glasgow, G12 8QQ, UK

\* E-mail address: [gz45@leicester.ac.uk](mailto:gz45@leicester.ac.uk)

### Supplementary information

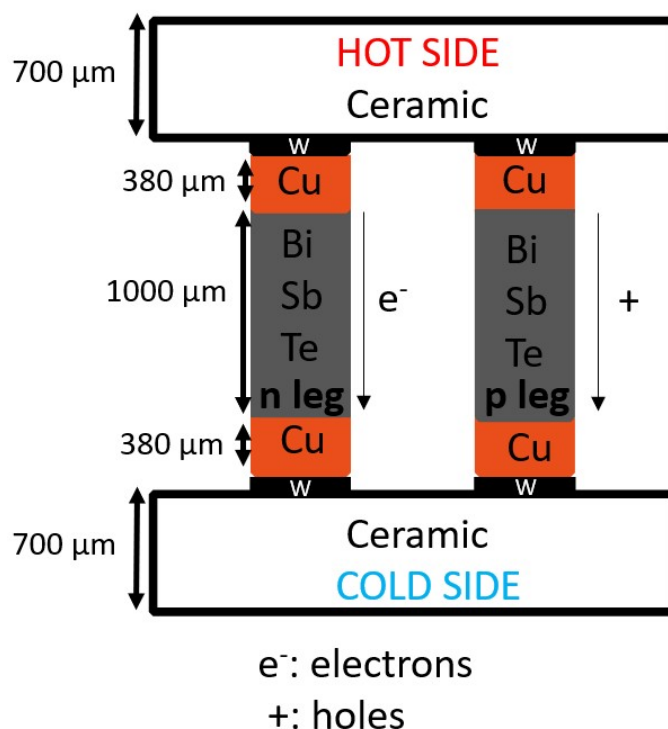


**Figure S1.** Structure of the thermoelectric material showing the ceramic plate, the 3  $\mu\text{m}$  thick W plate, Cu plate and  $\text{Bi}_{2-x}\text{Sb}_x\text{Te}_3$  thermoelectric legs. Solder layer on the W and Cu plate and thermoelectric leg is not represented.

$\text{Cu}^{\text{II}}$  forms different species when dissolved in aqueous salt solutions, from a hexaaqua complex in pure water, to a chloride complex in the most concentrated brines<sup>1</sup>. The  $\text{Cu}^{\text{II}}$  complexes formed will depend on the chloride ion concentration, the water concentration,

and the type of cation in the brine. Absorption spectra and photographs of Cu(II) chloride in the different brines are shown in **Figure S2**. Based on the absorbance maxima, predicted species can be found in **Table S1**.

Increasing the chloride content from  $1.0 \text{ mol}\cdot\text{kg}^{-1}$  to  $7.3 \text{ mol}\cdot\text{kg}^{-1}$  alters the speciation of the  $\text{Cu}^{\text{II}}$  ions in both series, from a greenish complex, to a yellowish complex. In ChCl brines with a chloride content of  $4.7$  and  $5.2 \text{ mol}\cdot\text{kg}^{-1}$ , three absorbance maxima are present at  $240$ ,  $285$ , and  $402 \text{ nm}$ , relating to the presence of  $[\text{CuCl}_4]^{2-}$  that is also known to form in  $\text{ChCl}: 2\text{EG}^{2,3}$ . At a chloride concentration of  $3.1 \text{ mol}\cdot\text{kg}^{-1}$ , three absorbance maxima are also present, but shifted to  $250$ ,  $278$ , and  $400 \text{ nm}$ . Comparing these spectra to those reported by De Vreese *et al.*<sup>4</sup>, the most likely species are a mixture of  $[\text{CuCl}(\text{H}_2\text{O})_n]^+$  and  $[\text{CuCl}_3(\text{H}_2\text{O})_n]^-$ , whereas the spectrum of  $\text{Cu}^{\text{II}}$  in a ChCl brine with a chloride concentration of  $1.0 \text{ mol}\cdot\text{kg}^{-1}$  only displays a single absorbance at  $250 \text{ nm}$ , indicating a possible mixture of  $[\text{CuCl}(\text{H}_2\text{O})_n]^+$  and  $[\text{Cu}(\text{H}_2\text{O})_n]^{2+}$ .

The speciation of  $\text{Cu}^{\text{II}}$  in the  $\text{CaCl}_2\cdot 6\text{H}_2\text{O}$  brines changes significantly with the chloride content. The absorbance maxima are present at  $274$  and  $383 \text{ nm}$  for chloride contents of  $5.0 \text{ mol}\cdot\text{kg}^{-1}$  and higher, and at  $250 \text{ nm}$  for a chloride content of  $1.8 \text{ mol}\cdot\text{kg}^{-1}$ , most likely relating to mixed chloride-aqua complexes. Hence, changing the chloride content and the salt of the brine greatly modifies the speciation of Cu in the solvent. This is likely due to the varying activity of water and chloride ions in these hypersaline solutions. Different cations can have varying degrees of attraction to water molecules, reducing the water activity, whilst other cations can dissociate more fully from the chloride anion, increasing chloride activity. For example, the  $\text{Cu}^{\text{II}}$  species present in a  $5.0 \text{ mol}\cdot\text{dm}^{-3}$  ( $3.9 \text{ mol}\cdot\text{kg}^{-1}$ ) sodium chloride brine<sup>1</sup> can be achieved with only  $3.1 \text{ mol}\cdot\text{kg}^{-1}$  ChCl or  $2.5 \text{ mol}\cdot\text{kg}^{-1}$   $\text{CaCl}_2\cdot 6\text{H}_2\text{O}$ , resulting in a decrease in the amount of chemicals required. The plot of the molar extinction coefficient at  $402 \text{ nm}$  as a function of water content in the brines is displayed in **Figure S3**. The plot is expected to be linear if the water activity decreases linearly. However, the plot for both brines is not linear, with  $R^2$  values below  $0.96$  for ChCl and below  $0.85$  for  $\text{CaCl}_2\cdot 6\text{H}_2\text{O}$  brines, respectively. A decrease of water content in both brines leads to a shift of the wavelength of the peaks, indicating that ligand exchange between water and chlorides is happening and that there is therefore no linear decrease of the concentration of species. The high ionic strength provided by DESs and ionic

liquids shields solute ions from each other, these solutes behaving independently from each other.<sup>5</sup> The nonlinear decrease of water activity seems to indicate that this assumption is not valid for brines or is only valid above a certain ionic strength/chloride concentration.

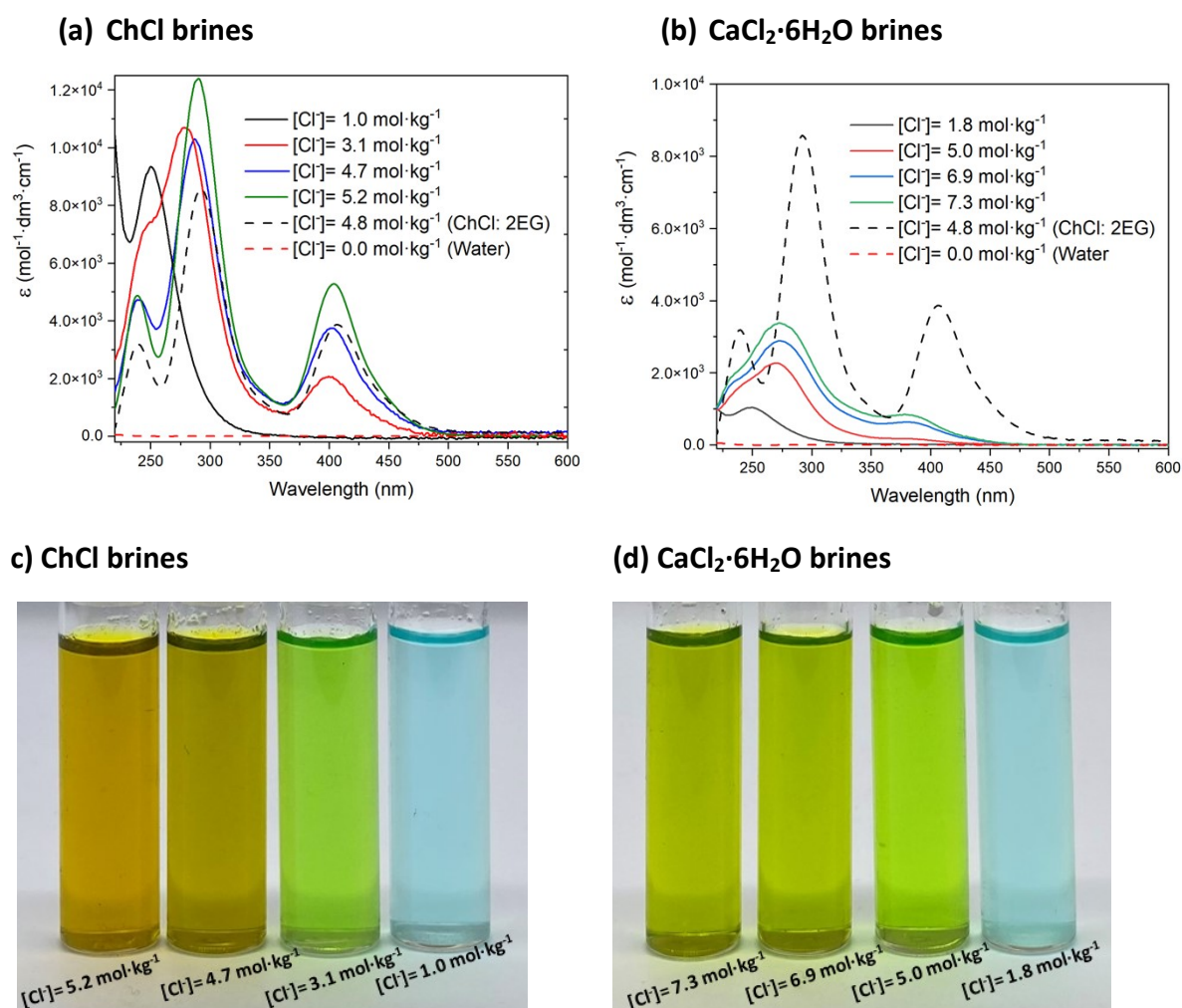


**Figure S2.** Molar extinction coefficient of Cu chloride dissolved in (a) ChCl brines, and (b)  $\text{CaCl}_2\cdot 6\text{H}_2\text{O}$  brines, and photographs of  $0.1 \text{ mol}\cdot\text{dm}^{-3}$   $\text{CuCl}_2$  dissolved in (c) ChCl brines, and (d)  $\text{CaCl}_2\cdot 6\text{H}_2\text{O}$  brines. The spectra of ChCl: 2EG and water are included for comparison.

**Table S1.** UV-vis absorbance maxima of the Cu<sup>II</sup> species present in the different chloride brines, along with the predicted species.

Solvent/Chloride content	Absorbances / nm	Predicted species
<i>CaCl<sub>2</sub>·6H<sub>2</sub>O brines</i>		
[Cl <sup>-</sup> ]= 7.3 mol·kg <sup>-1</sup>	274, 383	[CuCl <sub>3</sub> (H <sub>2</sub> O) <sub>n</sub> ] <sup>-</sup>
[Cl <sup>-</sup> ]= 6.9 mol·kg <sup>-1</sup>	274, 383	[CuCl <sub>3</sub> (H <sub>2</sub> O) <sub>n</sub> ] <sup>-</sup>
[Cl <sup>-</sup> ]= 5.0 mol·kg <sup>-1</sup>	274, 383	[CuCl(H <sub>2</sub> O) <sub>n</sub> ] <sup>+</sup> and [CuCl <sub>3</sub> (H <sub>2</sub> O) <sub>n</sub> ] <sup>-</sup>
[Cl <sup>-</sup> ]= 1.8 mol·kg <sup>-1</sup>	250	[CuCl(H <sub>2</sub> O) <sub>n</sub> ] <sup>+</sup>
<i>ChCl brines</i>		
[Cl <sup>-</sup> ]= 5.2 mol·kg <sup>-1</sup>	240, 285, 402	[CuCl <sub>4</sub> ] <sup>2-</sup>
[Cl <sup>-</sup> ]= 4.7 mol·kg <sup>-1</sup>	240, 285, 402	[CuCl <sub>4</sub> ] <sup>2-</sup>
[Cl <sup>-</sup> ]= 3.1 mol·kg <sup>-1</sup>	250, 278, 400	[CuCl(H <sub>2</sub> O) <sub>n</sub> ] <sup>+</sup> and [CuCl <sub>3</sub> (H <sub>2</sub> O) <sub>n</sub> ] <sup>-</sup>
[Cl <sup>-</sup> ]= 1.0 mol·kg <sup>-1</sup>	250	[CuCl(H <sub>2</sub> O) <sub>n</sub> ] <sup>+</sup> and [Cu(H <sub>2</sub> O) <sub>n</sub> ] <sup>2+</sup>
<i>Deep eutectic solvents</i>		
ChCl: 2EG ([Cl <sup>-</sup> ]= 3.8 mol·kg <sup>-1</sup> )	239.8, 291.8, 406.4	[CuCl <sub>4</sub> ] <sup>2-</sup>
CaCl <sub>2</sub> ·6H <sub>2</sub> O: 2EG ([Cl <sup>-</sup> ]= 5.7 mol·kg <sup>-1</sup> )	243.4, 282.6, 393.4	[CuCl <sub>4</sub> ] <sup>2-</sup>

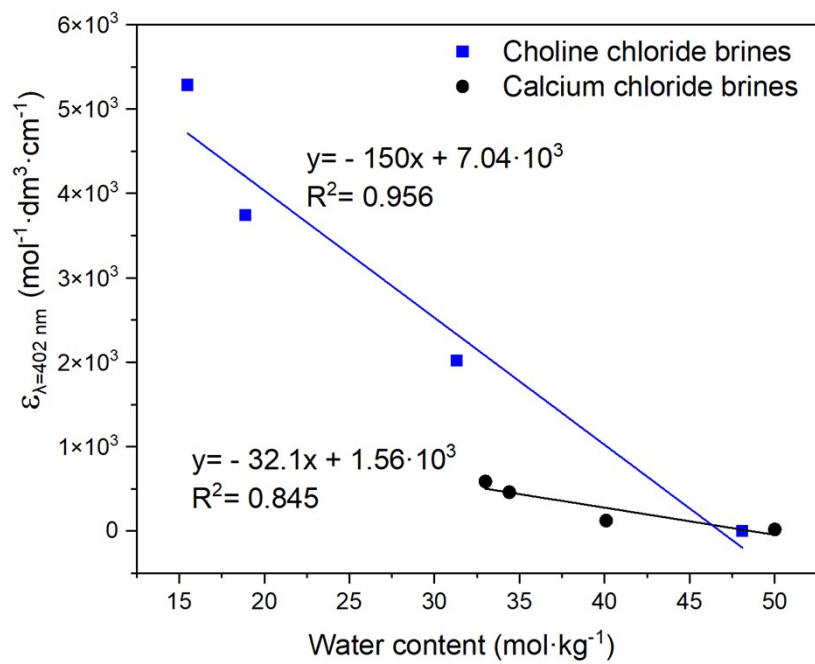


**Figure S3.** Molar extinction coefficient as a function of water content for Cu chloride dissolved in ChCl brines and CaCl<sub>2</sub>·6H<sub>2</sub>O brines (402 nm peak).

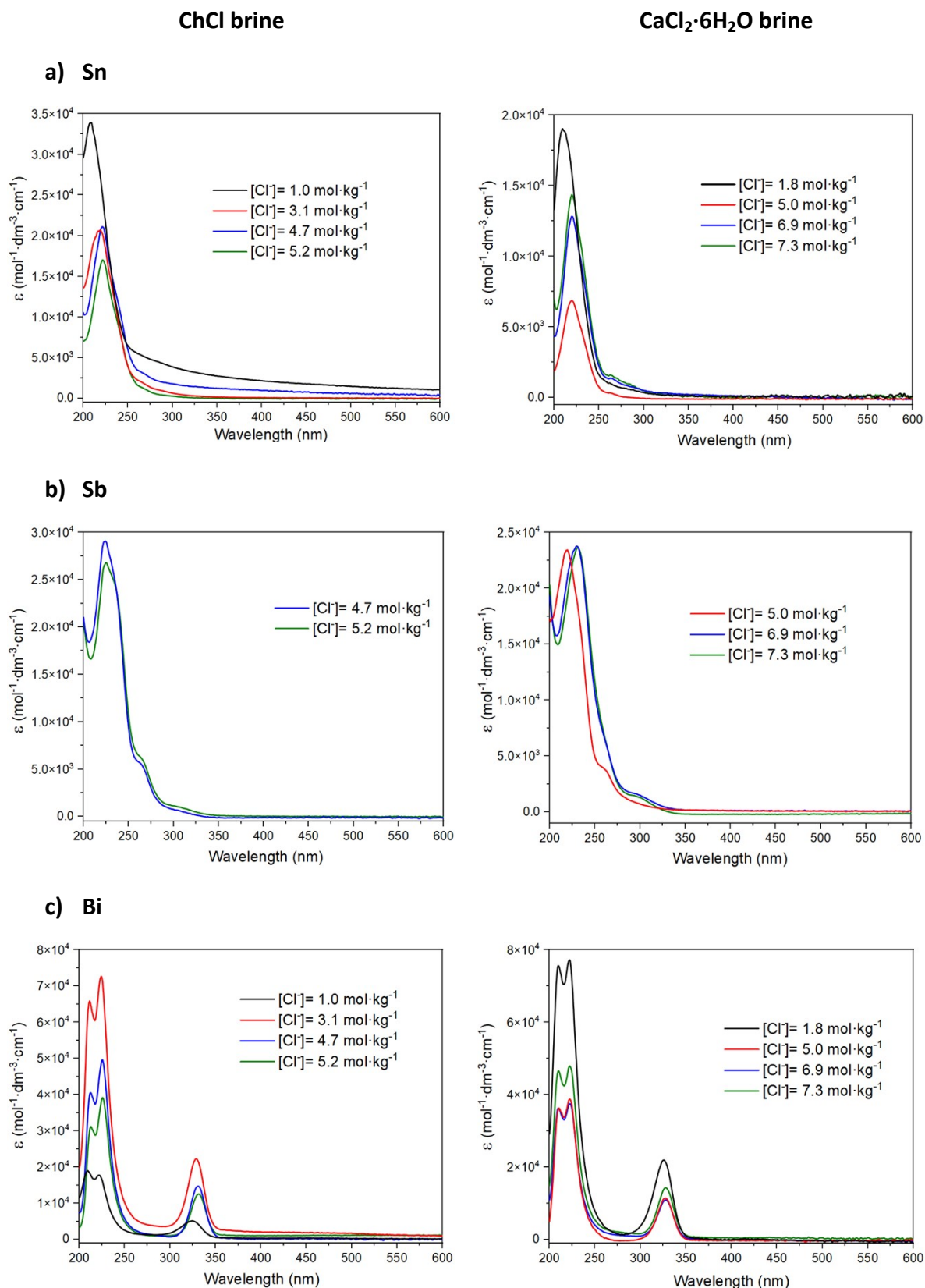


**Figure S4.** Molar extinction coefficient of metals chlorides dissolved in ChCl brines (left) and CaCl<sub>2</sub>·6H<sub>2</sub>O brines (right): a) Sn, (b) Sb, (c) Bi, and (d) Te.

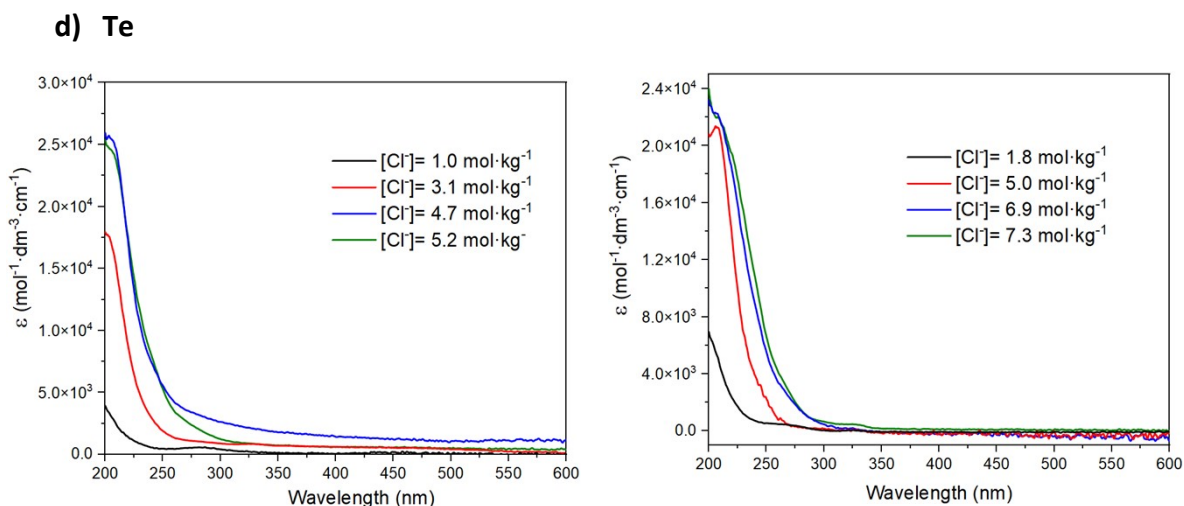


**Figure S4 (continued).** Molar extinction coefficient of metals chlorides dissolved in ChCl brines (left) and  $\text{CaCl}_2 \cdot 6\text{H}_2\text{O}$  brines (right): a) Sn, (b) Sb, (c) Bi, and (d) Te.

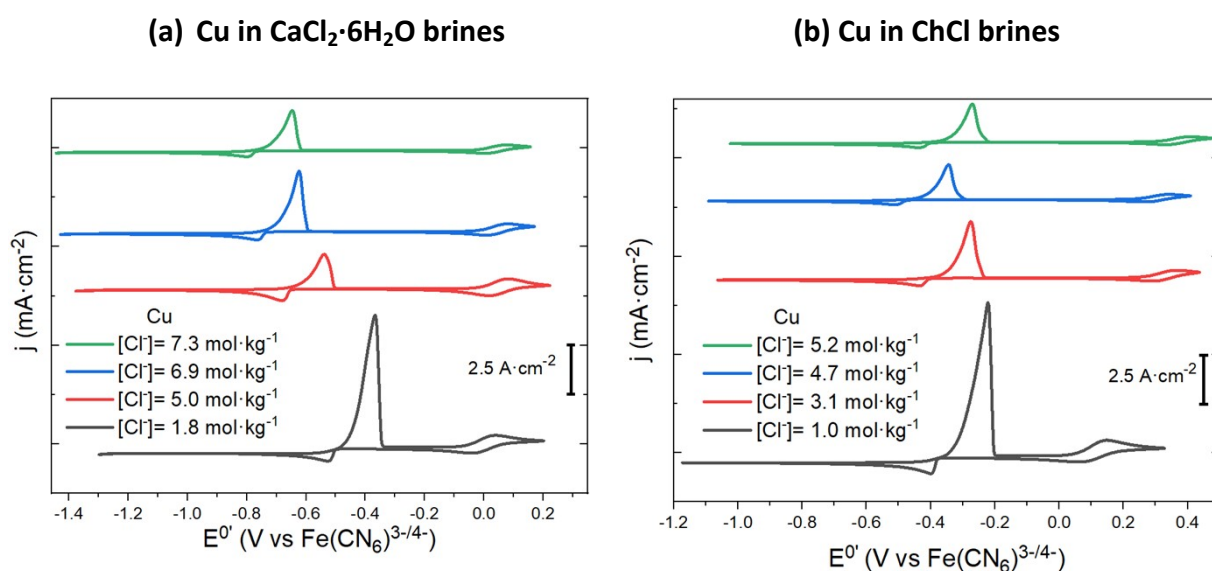
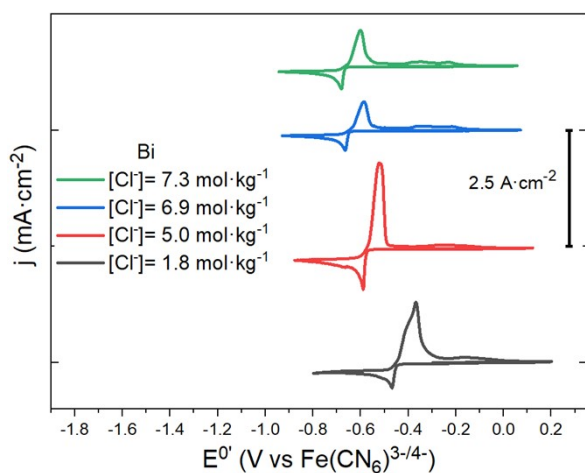
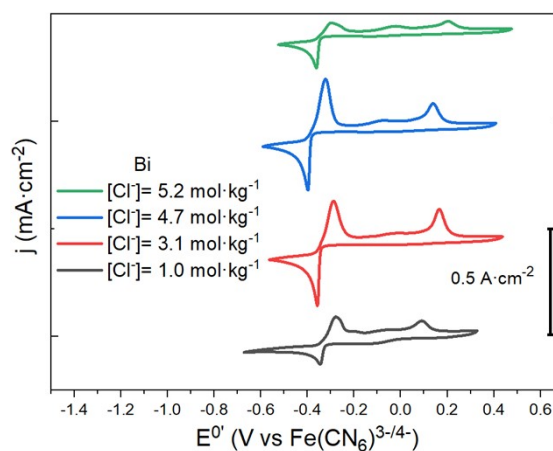


**Figure S5.** Cyclic voltammograms of  $0.02 \text{ mol dm}^{-3}$   $\text{Cu(II)}$  chloride in: (a)  $\text{CaCl}_2 \cdot 6\text{H}_2\text{O}$  and (b) ChCl brines, measured at a 1 mm diameter Pt-disc, with a scan rate of  $20 \text{ mV s}^{-1}$  and a temperature of  $25 \text{ }^\circ\text{C}$ . Potentials referenced to an internal standard of  $[\text{Fe}(\text{CN})_6]^{3-/4-}$ .

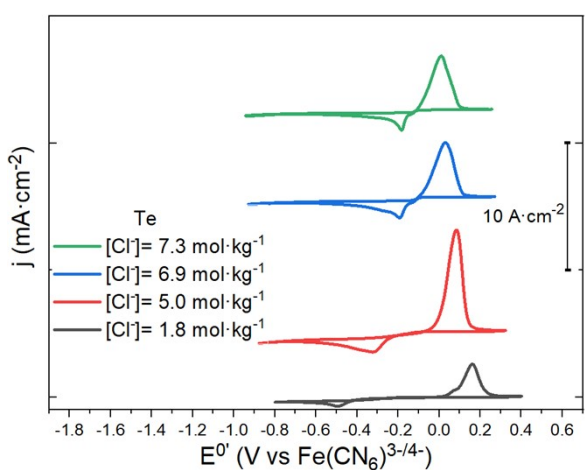
(a) BiCl<sub>3</sub> in CaCl<sub>2</sub>·6H<sub>2</sub>O brines



(b) BiCl<sub>3</sub> in ChCl brines



(c) TeCl<sub>4</sub> in CaCl<sub>2</sub>·6H<sub>2</sub>O brines



(d) TeCl<sub>4</sub> in ChCl brines

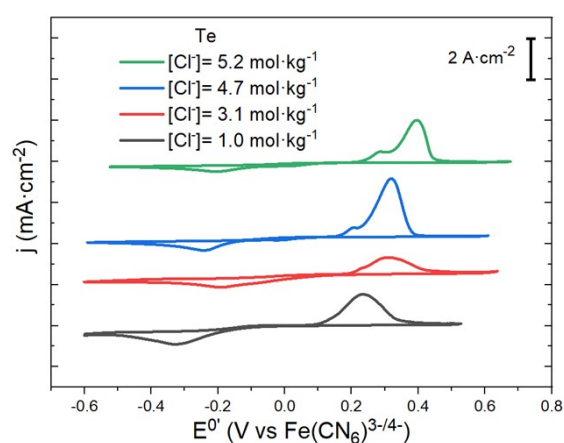
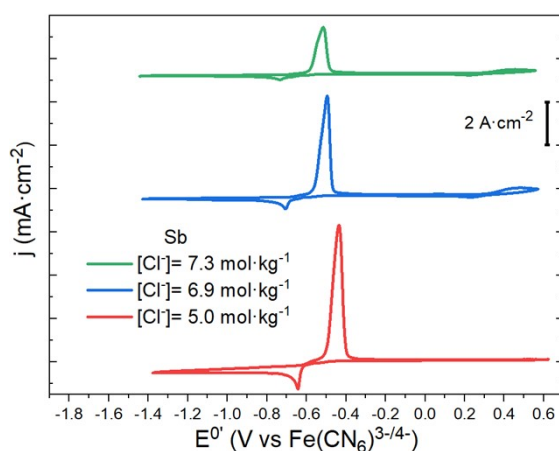
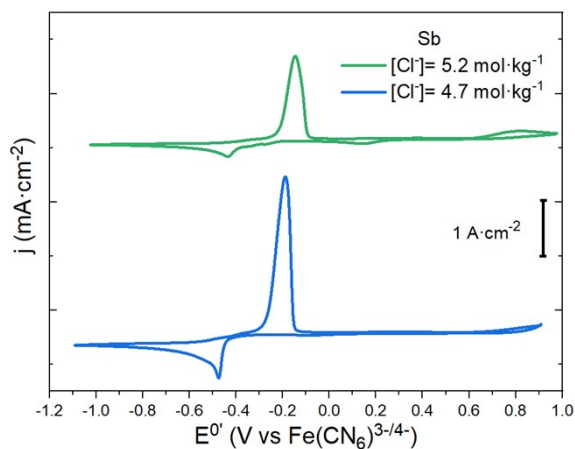


**Figure S6.** Cyclic voltammograms of Bi (III) chloride, Te(III) chloride, Sb(III) chloride and Sn(II) chloride in CaCl<sub>2</sub>·6H<sub>2</sub>O and ChCl brines, measured at a 1 mm diameter Pt-disc, with a scan rate of 20 mV s<sup>-1</sup> and a temperature of 25 °C. Potentials referenced to an internal standard of [Fe(CN)<sub>6</sub>]<sup>3-/4-</sup>.

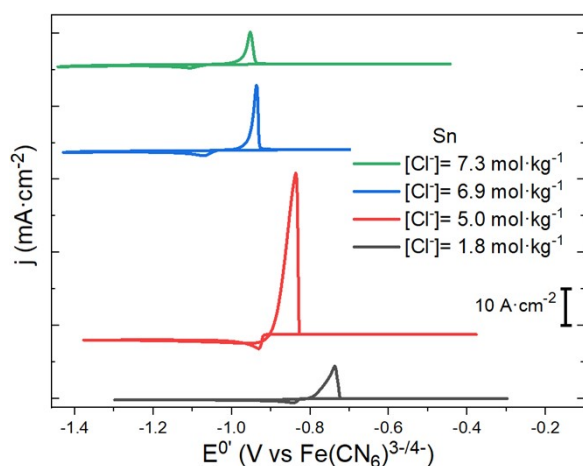
(e)  $\text{SbCl}_3$  in  $\text{CaCl}_2 \cdot 6\text{H}_2\text{O}$  brines



(f)  $\text{SbCl}_3$  in  $\text{ChCl}$  brines



(g)  $\text{SnCl}_2$  in  $\text{CaCl}_2 \cdot 6\text{H}_2\text{O}$  brines



(h)  $\text{SnCl}_2$  in  $\text{ChCl}$  brines

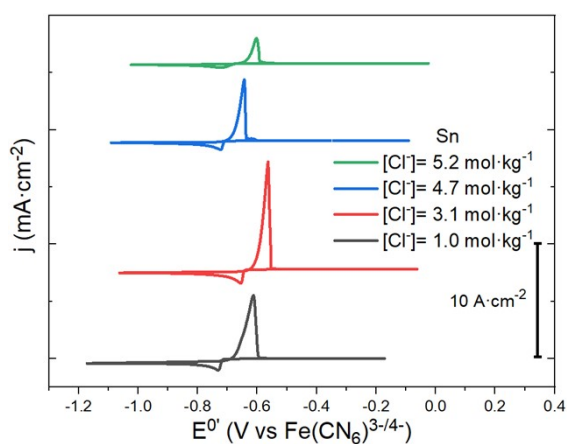


**Figure S6 (continued).** Cyclic voltammograms of Bi (III) chloride, Te(III) chloride, Sb(III) chloride and Sn(II) chloride in  $\text{CaCl}_2 \cdot 6\text{H}_2\text{O}$  and  $\text{ChCl}$  brines, measured at a 1 mm diameter Pt-disc, with a scan rate of  $20 \text{ mV s}^{-1}$  and a temperature of  $25 \text{ }^\circ\text{C}$ . Potentials referenced to an internal standard of  $[\text{Fe}(\text{CN})_6]^{3-/4-}$ .



**Figure S7.** Photograph of a ceramic plate after Cu removal (after repeated contacts with  $0.1 \text{ mol}\cdot\text{dm}^{-3}$  Cu(II) chloride in a ChCl brine containing  $1.0 \text{ mol}\cdot\text{kg}^{-1}$  chloride), revealing the grey W layer.

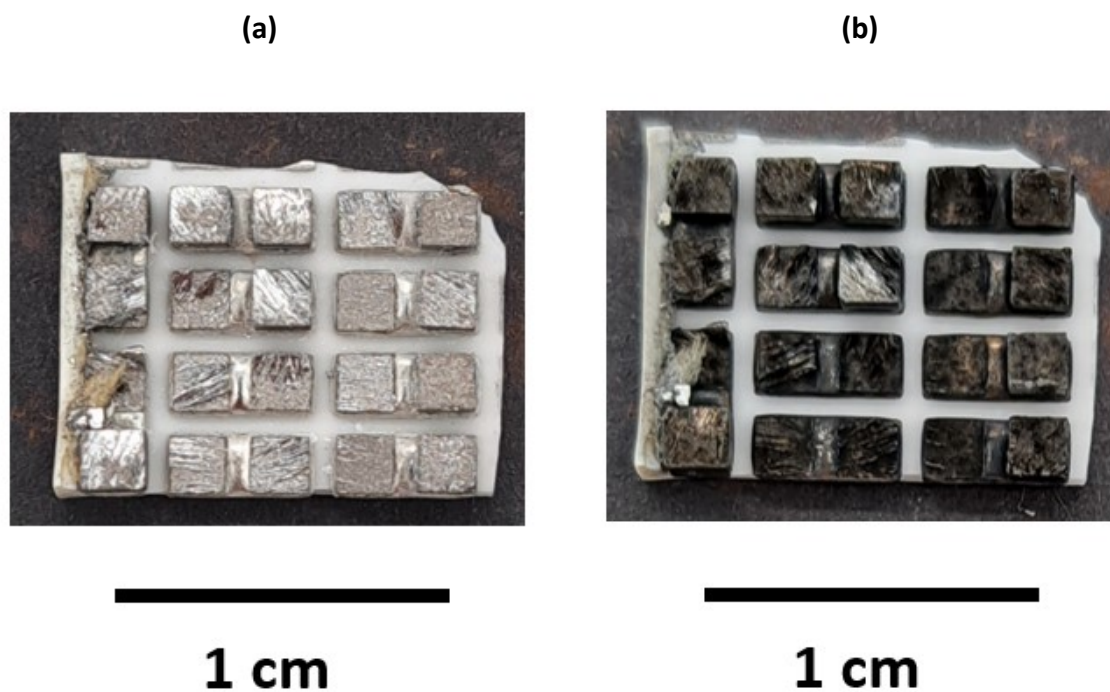


**Figure S8.** Photographs of a piece of thermoelectric (a) before, and (b) after solder dissolution with  $8 \text{ mol}\cdot\text{dm}^{-3}$  HCl in water.

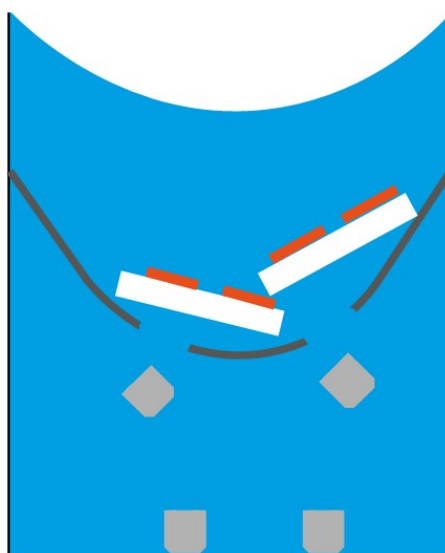


**Figure S9.** Scheme of the experimental device that will permit the recovery of ceramic (white rectangles), Cu (red rectangles) and  $\text{Bi}_{2-x}\text{Sb}_x\text{Te}_3$  (grey cubes) separately from thermoelectric materials. The sieve is depicted as a black curved dashed line, with the solvent in blue.

## References

- 1 M. D. Collings, D. M. Sherman and K. V. Ragnarsdottir, *Chemical Geology*, 2000, **167**, 65–73.
- 2 A. Y. M. Al-Murshedi, J. M. Hartley, A. P. Abbott and K. S. Ryder, *Transactions of the IMF*, 2019, **97**, 321–329.
- 3 J. M. Hartley, C.-M. Ip, G. C. H. Forrest, K. Singh, S. J. Gurman, K. S. Ryder, A. P. Abbott and G. Frisch, *Inorg. Chem.*, 2014, **53**, 6280–6288.
- 4 P. De Vreese, N. R. Brooks, K. Van Hecke, L. Van Meervelt, E. Mattheijs, K. Binnemans and R. Van Deun, *Inorg. Chem.*, 2012, **51**, 4972–4981.
- 5 A. P. Abbott, G. Frisch, H. Garrett and J. Hartley, *Chem. Commun.*, 2011, **47**, 11876.